Sinusoidal wavelength-scanning superluminescent diode interferometer for two-dimensional step-profile measurement

Osami Sasaki, Yasuhisa Shimakura, and Takamasa Suzuki

Niigata University, Faculty of Engineering
8050 Ikarashi 2, Niigata-shi 950-2181, Japan
Fax 81-25-262-6747 E-mail osami@eng.niigata-u.ac.jp

ABSTRACT

Two-dimensional step-profile measurement is carried out with a sinusoidal wavelength-scanning interferometer where a large scanning width of 41 nm is easily achieved using a superluminescent laser diode of a wide spectral bandwidth of 46 nm. To detect a time-varying interference signal with a short integration time of 118 μs, a shutter function of a two-dimensional CCD image sensor is utilized. A step profile with a step height of 1 μm is measured with an error less than a few nanometers. A Step profile with a step height of 20 μm is also measured with a scanning width of 23 nm.

Keywords: interferometer, wavelength-scanning, step-profile measurement, CCD image sensor

1. INTRODUCTION

Single-wavelength interferometers are limited to measurements of smooth and continuous surfaces on which a change of the optical path difference (OPD) between two measuring points is smaller than a wavelength. To overcome this limitation, two-wavelength interferometers[1-3], wavelength-scanning interferometers[4-10], and dispersive white-light interferometers[11-15] or white-light channelled spectrum interferometers have been developed. Among these interferometers, wavelength-scanning interferometers are the most useful and attractive if the wavelength of the light source can be scanned easily and exactly. Since measurement sensitivity in OPD is higher as the scanning width of wavelength is larger in wavelength-scanning interferometers, a light source with a large scanning width of wavelength is desirable.

A sinusoidal wavelength-scanning (SWS) light source using a superluminescent laser diode (SLD) was proposed and one-dimensional step-profile measurements were carried out with a linear CCD image sensor[10]. If this one-dimensional measurement is extended to two-dimensional measurement with a two-dimensional CCD image sensor, there are two problems to be solved. The SWS width of 13 nm in the one-dimensional measurement are not enough to measure an OPD from the phase-modulation amplitude Z_b with the measurement error less than a half wavelength. The reason is that signal-noise ratio in two-dimensional CCD image sensors is lower than that in linear CCD image sensors. The other problem is that a short integration time of a few hundreds μs and a high rate scan are needed for the detection of the interference signal with a two-dimensional CCD image sensor.

In this paper a SLD with a wide spectral bandwidth of 46 nm is used to achieve SWS width of 41 nm. A time-varying phase change of the interference signal due to the SWS contains sinusoidal phase-modulation amplitude Z_b and conventional phase α. To detect accurately the amplitude Z_b and the phase α, double sinusoidal phase-modulating interferometry[16] is used where another sinusoidal phase-modulation is added to the SWS. Maximum detectable value of Z_b is determined by the ratio of the SWS frequency to the sinusoidal phase-modulating frequency. We adjust the SWS width so that maximum measurable value of OPD becomes as large as possible within the maximum detectable value of Z_b. A two-dimensional CCD image sensor is used to make two-dimensional measurement. Since the interference signal varies with time and the sinusoidal phase-modulation

Advanced Materials and Devices for Sensing and Imaging, Jianquan Yao, Yukihiro Ishii, Editors, Proceedings of SPIE Vol. 4919 (2002) © 2002 SPIE · 0277-786X/02/$15.00

frequency is about 1 KHz, a short integration time of a few hundreds μs is required for the CCD image sensor. We utilize a shutter function of the CCD image sensor to realize the short integration time[19] and a high rate scan of the CCD image sensor to obtain a wide measuring region. The interference signals detected with the CCD image sensor are processed in a personal computer to obtain step-surface profiles.

After the principle of the SWS interferometer is reviewed, signal detection with a two-dimensional CCD image sensor is explained. In experiments, fundamental characteristics of the interferometer is examined and two-dimensional step-profile measurements are carried out for two different step heights of 1 μm and 20 μm.

2. SWS INTERFEROMETER USING A SLD

Figure 1 shows a SWS interferometer using a SLD for two-dimensional step-profile measurement. The output beam from the SLD is collimated with lens L1 and incident on diffraction grating G1. The first-order reflection from the grating is Fourier transformed with lens L2 to perform a grating spectroscope. A continuous spectrum of the SLD appears on the focal plane of lens L2 and L3. A central wavelength of the spectrum is λ_0. Slit SL, put on the focal plane, transmits a portion of the spectrum. The slit is connected with a magnetic coil of a speaker and vibrated sinusoidally with an angular frequency of ω_b. The central wavelength of the light passing through the slit is sinusoidally scanned, and it is expressed by

$$\lambda(t) = \lambda_0 + b\cos(\omega_b t)\,. \qquad (1)$$

The light coming out of the slit is Fourier transformed with lens L3 and incident on grating G2 so that the first-order reflection from the grating produces a collimated beam whose propagating direction is constant for all of wavelengths contained in the spectrum of the SLD. The collimated beam becomes an output of a SWS light source for an interferometer. The intensity of the beam changes with time, and it is denoted by $I_M(t)$.

The reference beam is reflected by a reference mirror that is vibrated by peizoelectric transducer PZT with a waveform of $a\cos\omega_c t$ to adapt double sinusoidal phase-modulating interferometry[16]. Denoting an OPD by L and using the condition of $b<<\lambda_0$ for approximating a phase of an interference signal, the interference signal is expressed as

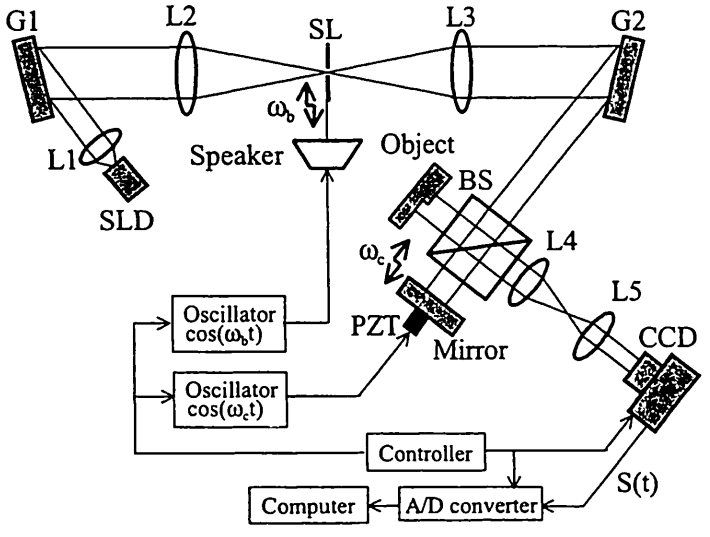

Fig.1 SWS interferometer using a SLD for step-profile measurement.

$$S(t) = I_M(t) [A+ B \cos(Z_c \cos\omega_c t + Z_b \cos\omega_b t + \alpha)], \quad (2)$$

where A and B are constants, $Z_c=4\pi a/\lambda_0$, and

$$Z_b=(2\pi b/\lambda_0^2)L , \quad (3)$$

$$\alpha=-(2\pi/\lambda_0)L . \quad (4)$$

By processing signal S(t) with the Fourier transform as has been described in Ref.14, we obtain

$$\phi(t) = Z_b \cos\omega_b t + \alpha . \quad (5)$$

Fourier-transform of $\phi(t)$ provides us values of Z_b and α. Since $Z_c \cos\omega_c t$ is a carrier signal for $\phi(t)$ and we use the Fourier transform, we have a relation of $\omega_c=2^p\omega_b$ where p is an integer. As the value of Z_b increases, the region where frequency components appear around an integral multiple of $\omega_c/2\pi$ becomes wider. Since the width of the region must be less than $\omega_c/2\pi$, maximum value of Z_b is limited to a specified value. When $\omega_c=16\omega_b$, value of Z_b must be less than about 6 rad.

We obtain a value of OPD from the value of Z_b that is denoted by L_z if the value of proportional constant $2\pi b/\lambda_0^2$ in Eq.(4) is known beforehand. We also obtain a fractional value of OPD from the value of α that is denoted by L_α. A value of L_α is in the range from $-\lambda_0/2$ to $\lambda_0/2$ and its measurement accuracy is a few nanometers. OPD L that represents the absolute distance is given by

$$L = m\lambda_0 + L_\alpha , \quad (6)$$

and we can obtain integer m by rounding off the following number to an integer if measurement error ε_{LZ} in L_z is smaller than $\lambda_0/2$:

$$m_c = (L_z - L_\alpha)/\lambda_0 . \quad (7)$$

In a SWS interferometer the combination of two measured values of L_z and L_α results in an exact OPD measurement over several tens of micronmeters with a high accuracy of a few nanometers.

3. SIGNAL DETECTION WITH A CCD IMAGE SENSOR

The frequencies of $f_b=\omega_b/2\pi$ and $f_c=\omega_c/2\pi=16f_b$ are 66.4 Hz and 1062.5 Hz, respectively. Signal S(t) is detected with a two-dimensional CCD image sensor. Integration time T_A of the CCD image sensor is taken to be $T_c/8=1/8f_c$.[17, 16] Since integration time is corresponding to frame period in CCD image sensors not equipped with a shutter function, the integration time of $T_A=T_c/8$ is very short for the CCD image sensors. If we utilize a shutter function of CCD image sensors, we can generate a short integration time within a frame period[19]. In order to detect eight different integrated values of S(t) with respect to one period T_c of signal $\cos(\omega_c t)$, frame period T_F is taken to be equal to $nT_c+ T_c/8$ and interference signal S(t) is integrated during the period of the shutter pulse equal to $T_A=T_c/8$. This timing is shown in Fig.2 in the case of n=2. The eight integrated values are detected in order of time with respect to the signal of $\cos(\omega_c t)$. The order of time is denoted by number of Q. The detection of the eight integrated values are repeated 16 times because of $f_c=16f_b$, so that 128 different integrated values of S(t) are detected at Q=0 to 127with respect to one period of $T_b=2\pi/\omega_b$ during the interval of 17 T_b. However 128 integrated values are not arranged in order of time with respect to the signal of $\cos(\omega_b t)$. We must rearrange the integrated values according to the order indicated by number

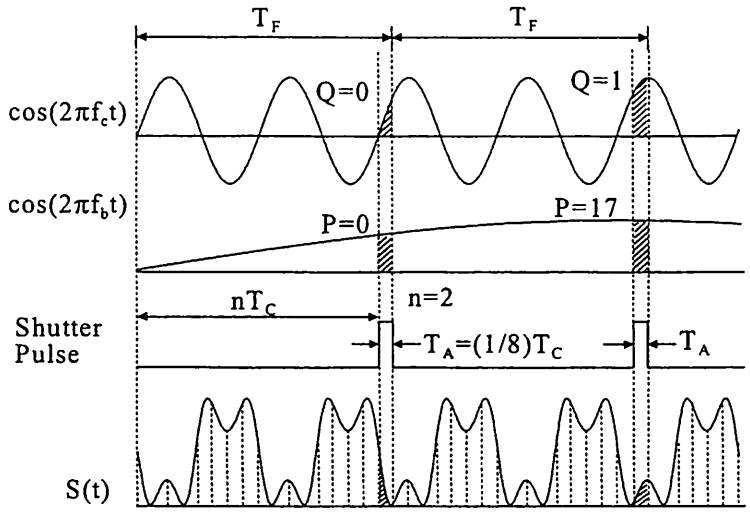

Fig.2 Timing of the integration of a CCD image sensor.

$$P=17Q-128\times IN[17Q/128], \quad (8)$$

where IN[y] means the integer portion of y. The same detection is repeated 8 times, which provides 128×8 values of the interference signal sampled at intervals of $T_c/8$.

4. EXPERIMENTS

4.1. Fundamental Characteristics

A SWS interferometer for two-dimensional step-profile measurement, as shown in Fig.1, was constructed. Central wavelength λ_0 and spectral bandwidth of the SLD were 830.3 nm and 46 nm, respectively. The width of the spectrum passing through the slit SL was about 6 nm. Lens 4 and 5 made an image of the object surface on the CCD image sensor with magnification of 1/2. We used n=2 and T_F=2 ms, and the CCD output the integrated values from 782×36 elements in horizontal and vertical direction, respectively. The output of the CCD only from 64×32 elements were A-D converted because of the limit of the memory size of the A-D converter. For one element we obtained 128×8 integrated values whose data length was $8T_b$.

A gauge block fixed on a stage was used as an object surface. We gave a displacement to the object by means of a micrometer to change the OPD at intervals of about 1 μm. Figure 3 shows values of Z_b measured for different values of change ΔL in OPD. For these measured values a linear line was fitted as shown in Fig.4, and we determined proportional constant D in the relationship of Z_b=DL. This determination of D was repeated and we obtained the values of D which were distributed between 0.186 rad /μm and 0.188 rad /μm. The average value D of 0.187 and the central wavelength λ_0 of 830.3 nm provided wavelength-scanning width 2b of 41.0 nm. The error ε_D in determination of 1/D was less than 0.03 μm/rad. We measured values of Z_b over the measuring region a few times. Figure 5 shows two kinds of measured values along one horizontal line, where the horizontal axis is the cell number I_x of the CCD image sensor along a horizontal line. The interval Δx between the two cells on the object surface was 33.2 μm, and the measuring region along the horizontal line was 33.2×62 μm. Since the object

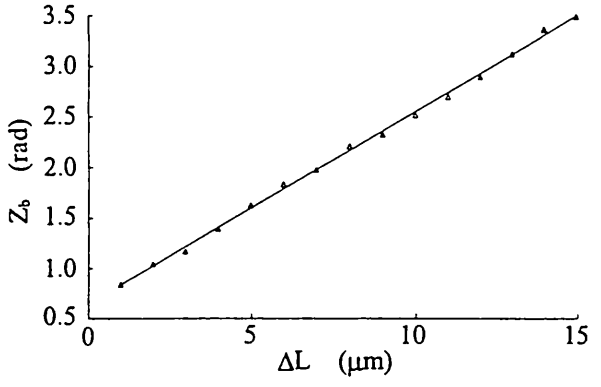

Fig.3 Values of Z_b measured for different values of change ΔL in OPD.

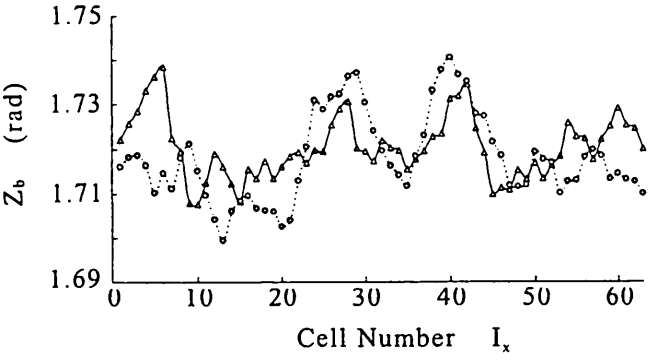

Fig.4 Variations of Z_b with time and space.

surface on the horizontal line was an optical flat, values of Z_b were expected to be on a straight line. These results indicate that measurement error ε_Z in Z_b caused by temporal and spatial variations was less than 0.02 rad. The measurement error ε_{LZ}, which is given by $(1/D)\varepsilon_Z + Z_b\varepsilon_D$, is must be less than $\lambda_0/2$ to combine two measured values of L_Z and L_α. This condition leads to the limitation that the measuring region of L is less that 55 μm in the conditions of D=0.187, ε_Z=0.02, and ε_D=0.03.

4.2. Step-Profile Measurement

We measured a step profile which was made by sticking two gauge blocks of different thickness together. The measured step profile is shown in Fig.5, where the difference between the two heights of the gauge blocks was 1μm in nominal value. I_x and I_y are the cell numbers of the two-dimensional CCD image sensor along the horizontal direction and vertical direction, respectively. Intervals Δx and Δy of the measuring points on the object surface along I_x and I_y were 33.2 μm and 16.6 μm, respectively. Size of the measuring region was 64×32 cells. Table 1 shows the measured values at some cells along one horizontal line of I_y=15. Exact measured values cannot be obtained at the cells of I_x=30-41around the boundary of the two gauge blocks, because light is strongly diffracted on the boundary. At the other cells differences between the value of m_c and an integer of its round

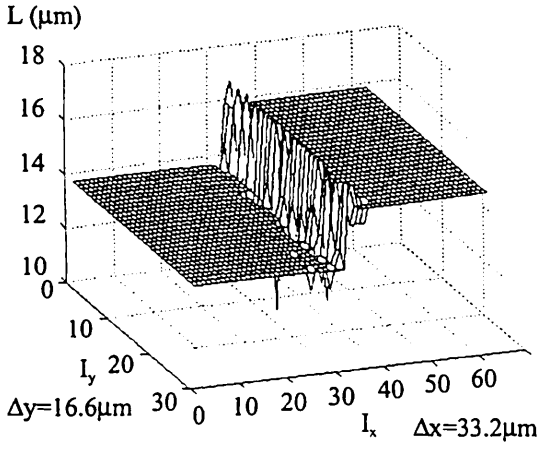

Fig.5 Measured result of step-surface profile with step height of 1 μm.

Table 1 Measured Values.

I_x	Z_b (rad)	L_z (μm)	α (rad)	L_α (μm)	m_c	L (μm)
20	2.559	13.83	2.20	-0.291	17.0	13.824
24	2.582	13.96	2.24	-0.296	17.2	13.819
28	2.592	14.01	2.29	-0.303	17.2	13.812
32	2.656	14.35	2.61	-0.345	17.7	14.600
36	2.844	15.37	-1.30	0.172	18.3	15.117
40	2.870	15.51	-1.21	0.160	18.5	15.105
44	2.898	15.67	-1.28	0.169	18.7	15.945
48	2.908	15.72	-1.37	0.181	18.7	15.957
52	2.923	15.80	-1.46	0.193	18.8	15.969

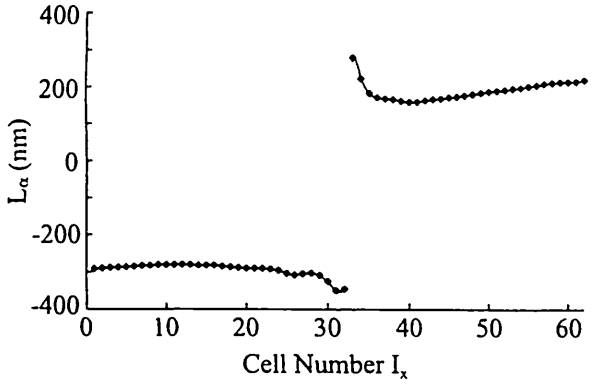

Fig.6 Measured result of L_α.

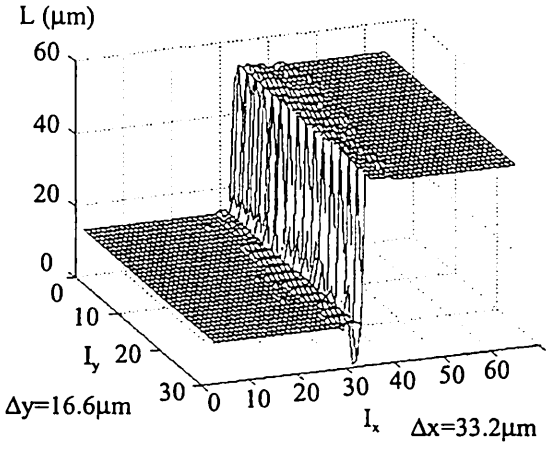

Fig.7 Measured result of step-surface profile with step height of 20 μm.

number are within 0.3. When we repeated the measurement, the distribution of m did not changed and the distribution of L_α changed within 3 nm. Distribution of L_α is shown in Fig.6 for the measurement whose results are shown in Table 1. An exact OPD can be obtained with the measurement error in L_α of about a few nanometers. The measured height of the step between cell 28 and 41 was 1.065 μm.

Next we tried to measure a step profile with a step height of 20 μm. If the wavelength-scanning width is still 41 nm, maximum value of Z_b becomes 7.5 rad in the relation of Z_b(rad)=0.187×L(μm). This value exceeds the maximum value of 6 rad described in Sec.2. Considering that the condition of $\varepsilon_{LZ}<\lambda_0/2$ had to be satisfied, we reduced the value of the wavelength-scanning width b. When 2b=23.0 nm, we obtained the relation of Z_b(rad)=0.105×L(μm). Value of L was 57 μm at Z_b=6 rad. The measured step profile with a step width of 20 μm is shown in Fig.7. The measurement errors in L_Z and L_α were the same as in the measurements of the object with the step height of 1 μm. The measured height of the step was 19.551 μm.

5. CONCLUSIONS

The SWS light source with the large scanning width of 41 nm was easily constructed using the SLD with the wide spectral bandwidth of 46 nm. This large SWS-width enabled us to make two-dimensional step-profile measurement. The shutter function of the two-dimensional CCD image sensor was utilized to detect the time-varying interference signal with the short integration time of 118 μs. And the short frame time of 2 ms was used to obtain 64×32 measuring points. The characteristics in detection of Z_b assured us that the combination of the two measured values L_Z and L_α were possible over the two-dimensional measuring region. A step profile with step height of 1 μm was measured with an error less than a few nanometers. For the measurement of a step profile with step height of 20 μm, the scanning width was reduced to 23 nm so that the value of Z_b was less than 6 rad. This measurement was also made with an error less than a few nanometers.

REFERENCES

1. P.de Groot and S.Kishner, "Synthetic wavelength stabilization for two-color laser-diode interferometry," Appl. Opt. 30, 4026-4033 (1991).
2. R.Onodera and Y.Ishii, "Two-wavelength laser-diode interferometer with fractional fringe techniques,"

Appl. Opt. 34, 4740-4746 (1995).
3. T.Suzuki, K.Kobayashi, and O.Sasaki, "Real-time displacement measurement with a two-wavelength sinusoidal phase-modulating laser diode," Appl. Opt. 39, 2646-2652 (2000).
4. H.J.Tiziani, B.Franze, and P.Haible, "Wavelength-shift speckle interferometry for absolute profilometry using mode-hope free external cavity diode laser," J. Mod. Opt. 44, 1485-1496 (1994).
5. S.Kuwamura, I.Yamaguchi, "Wavelength scanning profilometry for real-time surface shape measurement," Appl. Opt. 36, 4473-4482 (1997).
6. F.Lexer, C.K.Hitzenberger, A.F.Fercher, and M.Kulhavy, "Wavelength-tuning interferometry of intraocular distances," Appl. Opt. 36, 6548-6553 (1997).
7. T.Li, R.G.May, A.Wang, and R.O.Claus, "Optical scanning extrinsic Fabry-Perot interferometer for absolute microdisplacement measurement," Appl. Opt. 36, 8859-8861 (1997).
8. X.Dai, K.Seta, "High-accuracy absolute disatnace measurement by means of wavelength scanning heterodyne interferometry," Meas. Sci. Technol. 9, 1013-1035 (1998).
9. M.Kinoshita, M.Takeda, H.Yago, Y.Watanabe, and T.Kurokawa, "Optical frequency-domain microprofilometry with a frequency-tunable liquid-crystal Fabry-Perot etalon device," Appl. Opt. 38, 7063-7068 (1999).
10. O.Sasaki, N.Murata, and T.Suzuki, "Sinusoidal wavelength-scanning interferometer with a superluminescent diode for step-profile measurement," Appl. Opt. 39, 4589-4592 (2000).
11. J.Schwider and L.Zhou, "Dispersive interferometric profilometer," Opt. Lett. 19, 995-997 (1994).
12. U.Schnell, E.Zimmermann, and R.Dandliker, "Absolute distance measurement with synchronously sampled white-light channelled spectrum interferometry," Pure Appl. Opt. 4, 643-651 (1995).
13. P.Sandoz, G.Tribillon, and H.Perrin, "High-resolution profilometry by using phase calculation algorithms for spectroscopic analysis of white-light interferograms," J. of Mod. Opt. 43, 701-708 (1996).
14. L.Rovati, U.Minoni, and F.Docchio, "Dispersive white-light combined with a frequency-modulated continuous-wave interferometer for high-resolution absolute measurements of distance," Opt. Lett. 22, 850-852 (1997).
15. T.Funabe, N.Tanno, and H.Ito, "Multimode-laser reflectometer with a multichannel wavelength detector and its application," Appl. Opt. 36, 8919-8928 (1997).
16. O.Sasaki, T.Yoshida, and T.Suzuki, "Double sinusoidal phase-modulating laser diode interferometer for distance measurement," Appl. Opt. 30, 3617-3621 (1991).
17. O.Sasaki and H.Okazaki, "Detection of time-varying intensity distribution with CCD image sensors," Appl. Opt. 24, 2124-2126 (1986).
18. O.Sasaki and H.Okazaki, "Sinusoidal phase modulating interferometry for surface profile measurement," Appl. Opt. 25, 3137-3140 (1986).
19. T.Suzuki, T.Maki, X. Zhao and O.Sasaki, "Disturbance-free high-speed sinusoidal phase-modulating laser diode interferometer," Appl. Opt. 41, 1949-1953 (2002).